Measuring the Spatial Whole Transcriptome on FFPE specimens Using Digital Spatial Profiling: Analysis of Patients with Glioblastoma Multiforme Treated with Neoadjuvant Anti-PD1 Immunotherapy

ISB Science Transforming Health

nanoString®

NanoString Technologies 530 Fairview Avenue North, Seattle, WA 98109

Abstract

Glioblastoma (GBM) is the most common and most lethal malignant brain tumor with median survival of only 12 to 15 months. Although conventional and immunotherapies have yielded only marginal significant improvements in the overall survival of patients with GBM, recent neoadjuvant anti-PD-1 (Keytruda) immunotherapy resulted in promoting a survival benefit in patients with recurrent GBM. Bulk RNA assessment of tumor resections revealed that the neoadjuvant treatment was associated with upregulation of T-cell and IFN-γ-related genes, and downregulation of cell cycle-related genes. However, the tissue-level origin of these observations is unclear due to the lack of spatial information. Here, we employ Nanostring's GeoMx® Digital Spatial Profiling platform (GeoMx-DSP) to spatially resolve the whole transcriptome in 5-µm FFPE tissue specimens. This technology enabled us to spatially resolve the signaling pathways and transcripts that determine molecular response to immunotherapy.

GeoMx-DSP chemistry and workflow

Concept

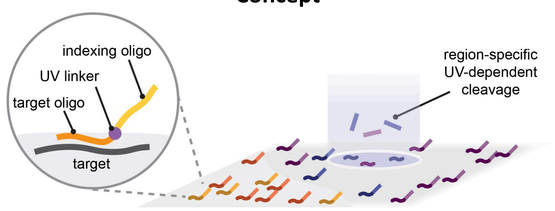

Workflow

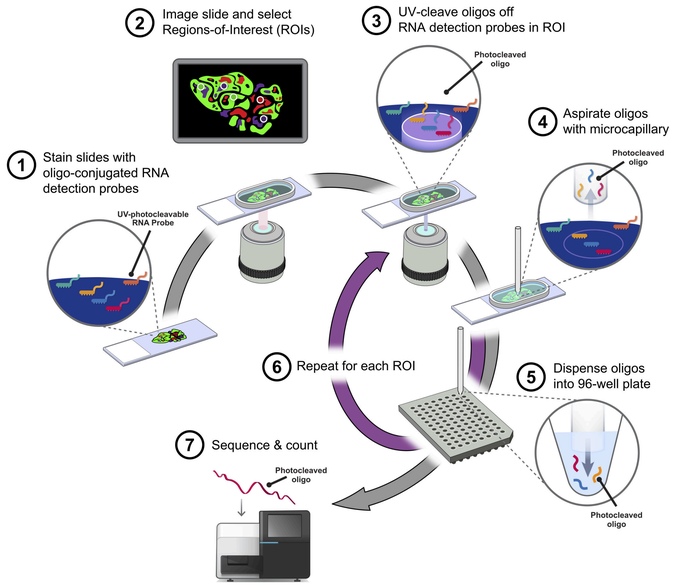

Whole Transcriptome Atlas (WTA)

- Designed to target all human protein-coding genes
- Curated to reduce signal from off-target hybridization, redundant target binding, mitochondrial genes, and high expressors
- 136 ERCC probes added as negative controls to measure background in the assay
- Final list of 18507 probes detects 19365 targets
- Focus on dynamic range: **targeted design emphasizes biologically important genes and ensures sensitivity for even low expressors**

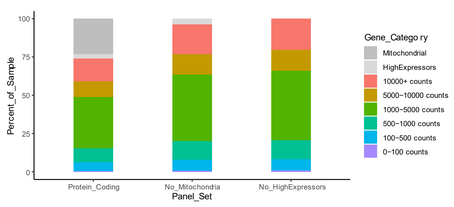

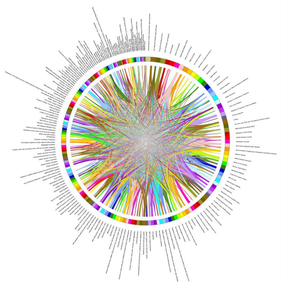

WTA pathway content; connections between annotations represent shared gene content exceeding 15 genes.

Technical QC for WTA GeoMx-DSP experiments

Sequencing metrics across all WTA GeoMx-DSP runs:

- AOI aspirate was sequenced at a depth of 112 reads/µm², achieving a mean sequencing saturation of 75% (25% unique reads)
- 15,109 genes were detected above LOD in at least one segment

Genes above LOD per AOI for each sample, stratified by CD45 status

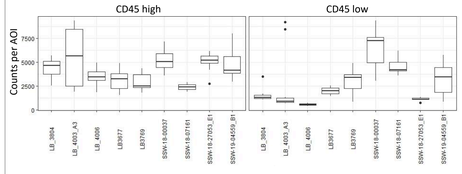

Stratifying the samples by CD45 status reveals that AOIs collected from CD45 low areas often exhibit fewer genes detected per AOI. This observation indicates that these AOIs contain lower levels of cell-type heterogeneity.

Technical validation: Correlation between CD45 signal – RNAscope™ and GeoMx-DSP

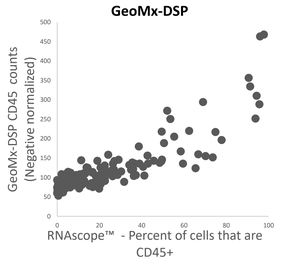

Scatter plot of normalized CD45 counts measured by GeoMx-DSP versus the percent of cells that are CD45+ as measured by RNAscope™ labeling.

Visualization markers enable targeted, informed AOI selection in GBM samples

- RNAscope was used to label CD45 (magenta) and Ki67 (green) transcripts. CD45 identifies Immune cell rich regions, Ki67 identifies proliferating cells
- AOIs were collected from regions manually classified as CD45-, CD45+, or CD45++
- 13 slides were analyzed
- 154 AOIs, classified as CD45- (44), CD45+ (77), and CD45++ (33), were sequenced
- An automated nuclei segmentation program was used to facilitate classification into CD45 positive or CD45 negative categories. For all analyses, AOIs were labeled as CD45 high or CD45 low, based on a cutoff of 12%, with a total of 80 CD45 high AOIs and 74 CD45 low AOIs.

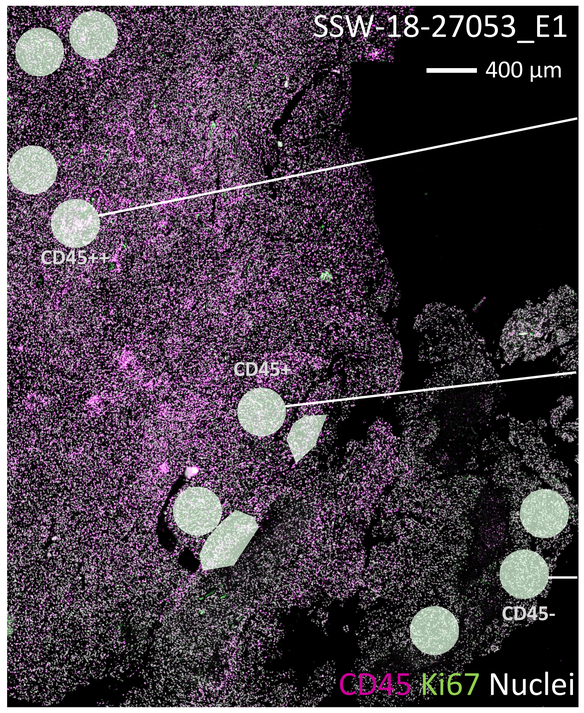

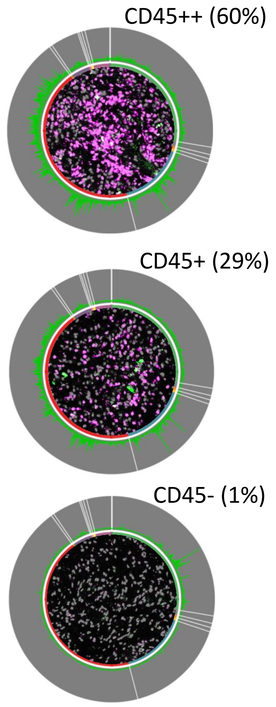

Representative image of CD45 (magenta) and Ki67 (green) transcripts as labeled by RNAscope. AOIs collected in this experiment are shaded, and representative AOIs from the CD45 expression categories are shown on the right. Each AOI's gene expression profile is shown as a circle plot surrounding the corresponding AOI. The number in parentheses reports the percentage of CD45+ cells measured by the automated quantification

CD45+/- and Responder/Non-Responder comparisons uncover potential genes and pathways involved in response to neoadjuvant anti-PD1 treatment of GBM

Differential expression between CD45 high/low ROIs and Responder/Non-Responder patient status identifies gene clusters

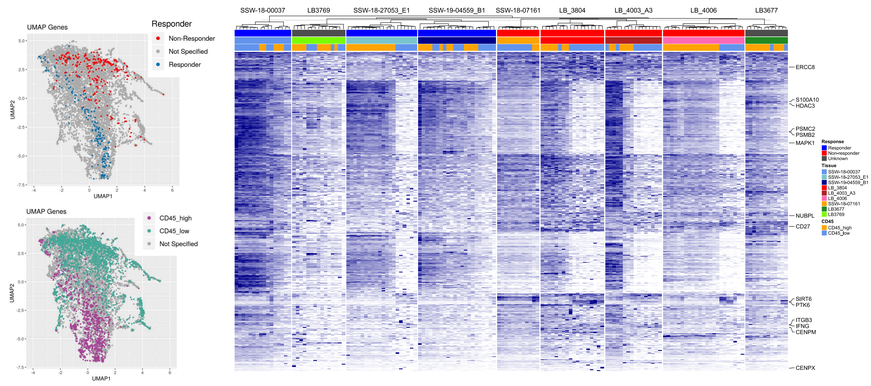

AOIs were annotated by CD45 level and clinical categorization of Responder/Non-Responder status (determined from bulk tumor RNA profiling utilizing the NanoString nCounter® PanCancer IO360™ panel). Within these categories, relevant genes were identified based on differential expression pval < 0.05. On left, each point is a gene in UMAP space and genes with similar expression patterns across AOIs are grouped together. Genes enriched in chosen conditions are annotated on the plot (top: Responder/Non-Responder; bottom: CD45 high/low). On right, heatmap shows expression of 416 top differentially-expressed genes in Responder/Non-Responder comparison. AOIs within each sample are arranged with hierarchical clustering.

Volcano plots highlight pathways that affect treatment response in CD45 high and low regions

CD45 low AOIs

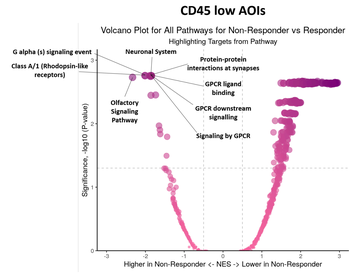

CD45 high AOIs

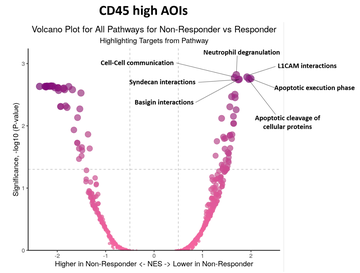

Top Gene Set Enrichment Analysis (GSEA) pathway hits based on differential gene expression of responders in CD45 low (left) and high (right) AOIs. Expected pathways are identified (eg GPCR signaling), prompting further questions about particular genes driving the pathway identification.

Identified pathways may suggest genes involved in response to anti-PD1 treatment

CD45 low AOIs, GPCR signaling genes

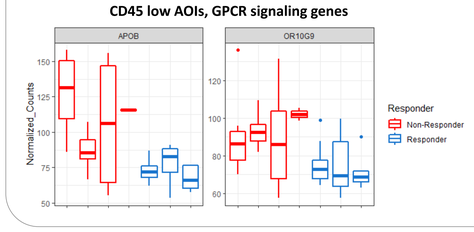

CD45 high AOIs, L1CAM interaction genes

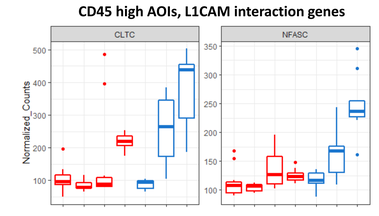

Cell mixture deconvolution facilitates a map of Tumor Infiltrating Lymphocytes across tissues

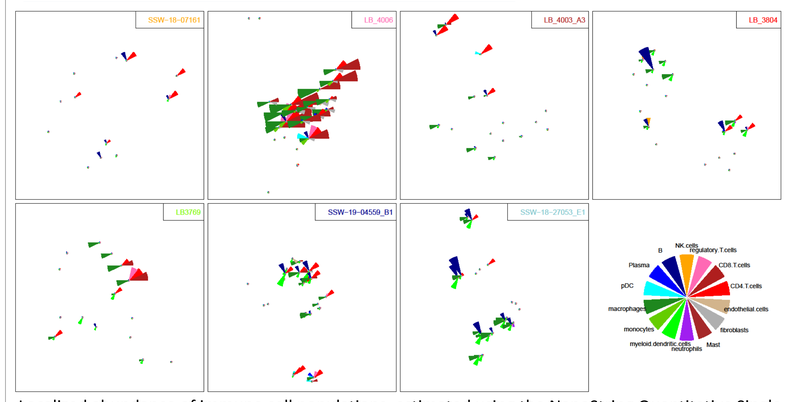

Localized abundance of immune cell populations, estimated using the NanoString Quantitative Single Cell Deconvolution algorithm. Spatial layout maintains AOI X/Y coordinates of the sample slide.

Clustering of the localized immune infiltrate. Identifiable clusters include regions dominated by macrophages, by T-cells, and by a mix of the two.

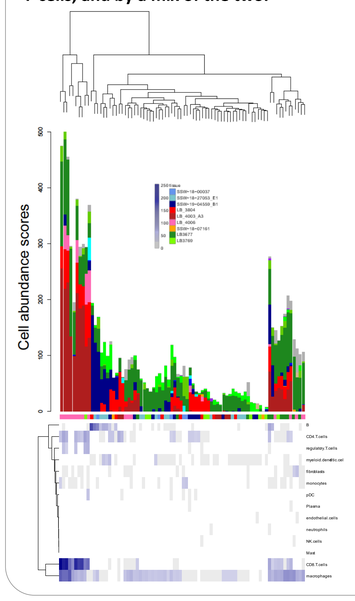

Macrophage- and T-cell-dominated regions are associated with distinct expression programs

Delineation of macrophage- and T-cell-dominated regions

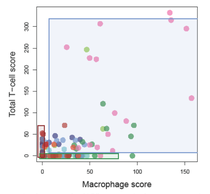

Transcriptome-wide associations with macrophage- and T-cell-dominated regions

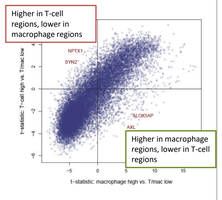

Selected differential expression results: expression of neuron-specific genes (NPTX1 and SYN2) is enriched in T-cell-dominated regions and depleted in macrophage-dominated regions. Macrophage-rich regions have elevated expression of the immune escape gene AXL and the inflammation mediating gene ALOX5AP.

Co-expression networks reveal intra-patient gene modules

Co-expression network in CD45 high AOIs

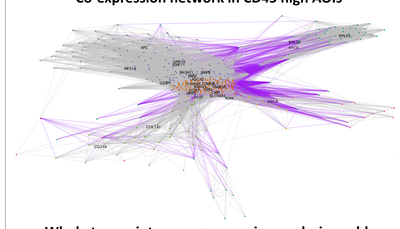

Co-expression network in CD45 low AOIs

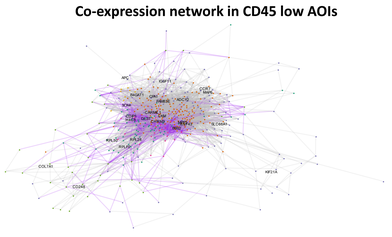

Whole transcriptome co-expression analysis enables exploration into tumor heterogeneity: 49357 edges and 411 genes pass threshold to create network that describes within-patient co-expression relationships across AOIs. Co-expression network representing the within-patient precision matrix. Node color denotes cluster assignment; names show genes that are most representative of their cluster; purple edge denotes negative correlation, grey edge denotes positive correlation.
Each edge in co-expression network represents a gene pair relationship that can be further analyzed.

Key immunology genes track differently depending on AOI type

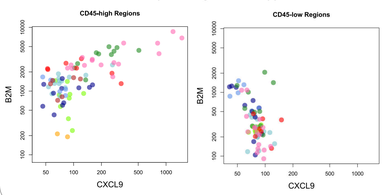

Immune and apoptosis genes track similarly in different AOI types

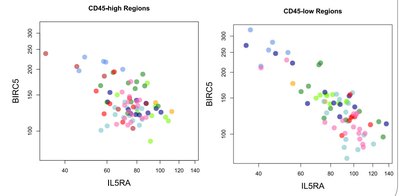

Conclusions

Sampling only tens of AOIs across each FFPE specimen, WTA GeoMx-DSP recapitulates the bulk signatures of immunotherapy response, as well as spatially resolving those signatures to specific cellular compartments of the tumor microenvironment. The technique also reveals signaling pathways and transcripts that determine response, and suggests several new avenues of clinical and scientific investigation into GBM.

Researchers interested in participating in NanoString's technology access program for its Digital Spatial Profiling technology should contact us at TAP@nanostring.com.

Yue Lu[1], Alphonsus Ng[1], Bridget Kulasekara[2], Maddy Griswold[2], Nileshi Saraf[2], Patrick Danaher[2], Lei Yang[2], Robin Fropf[2], Timothy F Cloughesy[3], Robert M Prins[3], Michael Rhodes[2], Joseph Beechem[2], Jim Heath[1]

1 – Institute for Systems Biology; 2 – NanoString Technologies; 3 – University of California, Los Angeles

AGBT, February 23rd – 26th, 2020